ISSN 0020-1685, Inorganic Materials, 2017, Vol. 53, No. 12, pp. 1270–1278. © Pleiades Publishing, Ltd., 2017.
Original Russian Text © S.A. Lermontov, A.N. Malkova, N.A. Sipyagina, Kh.E. Yorov, G.P. Kopitsa, A.E. Baranchikov, V.K. Ivanov, V. Pipich, N.K. Szekely, 2017, published in Neorganicheskie Materialy, 2017, Vol. 53, No. 00000, pp. 00000–00000.

Comparative Analysis of the Physicochemical Characteristics of SiO_2 Aerogels Prepared by Drying under Subcritical and Supercritical Conditions

S. A. Lermontov[a, *], A. N. Malkova[a], N. A. Sipyagina[a], Kh. E. Yorov[b], G. P. Kopitsa[c, d], A. E. Baranchikov[b, e], V. K. Ivanov[e, f], V. Pipich[g], and N. K. Szekely[g]

[a] *Institute of Physiologically Active Compounds, Russian Academy of Sciences, Severnyi proezd 1, Chernogolovka, Noginskii raion, Moscow oblast, 142432 Russia*

[b] *Moscow State University, Moscow, 119991 Russia*

[c] *Konstantinov Institute of Nuclear Physics, Kurchatov Institute National Research Center, Orlova Roshcha 1, Gatchina, Leningrad oblast, 188300 Russia*

[d] *Grebenshchikov Institute of Silicate Chemistry, Russian Academy of Sciences, nab. Makarova 2, St. Petersburg, 199034 Russia*

[e] *Kurnakov Institute of General and Inorganic Chemistry, Russian Academy of Sciences, Leninskii pr. 31, Moscow, 119991 Russia*

[f] *National Research Tomsk State University, pr. Lenina 36, Tomsk, 634050 Russia*

[g] *Jülich Centre for Neutron Science Outstation at MLZ, Lichtenbergstrasse 1, 85747 Garching, Germany*

**e-mail: lermon52@yandex.ru*

Received February 2, 2017

Abstract—SiO_2-based aerogels have been produced be removing a solvent (ethanol or hexafluoroisopropanol) from lyogels both above and below the critical temperature of the alcohols (in the range 210–260 and 160–220°C, respectively). The resultant materials have been characterized by low-temperature nitrogen adsorption measurements, X-ray diffraction, thermal analysis, scanning electron microscopy, X-ray microanalysis, and small-angle and ultrasmall-angle neutron scattering. The results demonstrate that removing the solvent 20–30°C below the critical temperature of the solvent yields silica that is characterized by higher specific porosity and has the same or a larger specific surface area in comparison with the aerogels produced by drying under supercritical conditions. The nature of the solvent used and the solvent removal temperature influence the size and aggregation behavior of primary clusters and the cluster aggregate size in the aerogels.

Keywords: aerogels, supercritical drying, subcritical drying, mesostructure, specific surface area

DOI: 10.1134/S002016851712007X

INTRODUCTION

Aerogels constitute a class of unique materials having low density, large specific surface area, and high porosity, which has opened up a wide variety of possible practical applications for them as sorbents, heterogeneous catalyst supports, photocatalysts, sensors, components of electrochemical systems, heat and sound insulators, etc. [1–8].

To date, a number of methods have been proposed for the synthesis of aerogels of various chemical compositions, based on individual and binary oxide compounds of metals and silicon (for example, SiO_2 [9], V_2O_5 [10], VO_x [11], TiO_2 [12], TiO_2–SiO_2 [13–15], $V_xTi_{1-x}O_y$ [16], and ZrO_2–SiO_2 [17]), organic compounds, hybrid organic–inorganic materials [18, 19], carbon nanostructures [20, 21], and many others.

A key step in the preparation of metal oxide aerogels, determining their physicochemical properties of practical importance, is solvent removal. In this step, capillary forces in the gel matrix produce mechanical stress, which may lead to complete disintegration of the gel structure, shrinkage, cracking, and fragmentation. Traditionally, aerogels are produced using supercritical drying (solvent removal at temperatures and pressures above the critical parameters), which makes it possible to almost completely avoid the formation of liquid–solid interfaces and considerable mechanical stress in the gel. Note that, in recent years, considerable attention was paid to an approach that allows one to obtain monolithic aerogels by removing the solvent at atmospheric pressure and relatively low temperatures (ambient pressure drying), which includes a steplike exchange of the solvent filling the gel pores for a solvent having as low surface tension as possible, or

via chemical modification of the surface of a metal–oxide matrix in order to make it hydrophobic [22–25].

The most widespread approach to the preparation of oxide aerogels includes the hydrolysis of metal and/or silicon alkoxides in alcohol-containing (methanol, ethanol, or isopropanol) solutions, which determines the supercritical drying conditions for the resultant lyogels: the process should be run at temperatures well above the critical one (t_c): 243°C for ethanol, 239°C for methanol, and 235°C for isopropanol. There are published data on the effect of supercritical solvent removal conditions on the physicochemical properties of the resultant aerogels [26–29] (in particular at pressures below the critical one [26]), but the effect of gel drying temperature near the critical one has not yet been analyzed.

The purpose of this work was to study in detail the physicochemical characteristics of SiO_2 aerogels prepared by drying both above and below the critical temperature of different solvents (ethanol and hexafluoroisopropanol).

EXPERIMENTAL

Aerogel synthesis. The starting chemicals used were tetraethyl orthosilicate (TEOS) (Aldrich, 99%), hydrofluoric acid (aqueous 40% solution, Aldrich), ethanol (Aldrich, 99%), and hexafluoroisopropanol (HFIP) (P&M Invest, Russia, 99+%).

SiO_2 lyogels were synthesized through TEOS hydrolysis by a modified technique [30]. To a solution containing TEOS (6 mL, 0.027 mmol) and ethanol (4.7 mL, 0.081 mol) and cooled to 3–5°C was added a solution prepared by mixing an aqueous 40% HF solution (0.054 g, 0.0011 mol) and distilled water (1.9 mL, 0.108 mol), also cooled to 3–5°C. The resultant mixture was stirred until a transparent solution was obtained (1 min), which was then transferred to a 15-mL cylindrical plastic container and left to stand for 24 h at room temperature, which resulted in gel formation and aging. The resultant gel was placed in a larger container and washed. To this end, an excess of a solvent (ethanol or hexafluoroisopropanol) was added to the gel in the container, which was then left to stand for 24 h, following which the solvent was decanted. The washing step was repeated five times. Next, the solvent was removed at temperatures of 210, 240, and 260°C if ethanol was used or at 160, 190, and 220°C in the case of HFIP. The solvent removal temperature was chosen so that it was 20–30°C above or below the critical temperature or roughly coincided with it. For drying, the gels and the corresponding solvent (14–16 mL) were placed in 40-L steel autoclaves and heated to a preset temperature over a period of 1.5–2 h. After the preset temperature was reached, the valves of the autoclaves were opened and the pressure was lowered to 1 atm over a period of 2 h. Next, the heated autoclaves were pumped down to a pressure of 1–1.2 kPa over a period of 30 min, cooled to room temperature, and opened.

Characterization techniques. Using low-temperature nitrogen adsorption measurements with ATKh-06 analyzer (KATAKON, Russia), we determined the specific surface area of the aerogels and constructed full nitrogen adsorption/desorption isotherms. Prior to the measurements, the samples were degassed in a flow of a dry helium–nitrogen mixture at 200°C for 30 min. From the data thus obtained, we evaluated the specific surface area of the samples in the BET model, using five data points at partial pressures in the range 0.05–0.25. The pore size distribution was assessed by the Barrett–Joyner–Halenda method using desorption isotherms.

The samples were characterized by thermogravimetry (TG) and differential thermal analysis (DTA) during heating to 800°C at a constant rate (3°C/min) in flowing synthetic air (100 mL/min) using an SDT Q-600 TGA/DSC/DTA integrated system (TA Instruments).

The percentage of fluorine in the aerogel samples was evaluated by X-ray microanalysis on a Carl Zeiss NVision 40 high-resolution scanning electron microscope equipped with an Oxford Instruments X-Max energy dispersive X-ray detector (80 mm^2), at an accelerating voltage of 20 kV. Scanning electron microscope images of the samples were obtained at an accelerating voltage of 1 kV.

The phase composition of the samples was determined by X-ray diffraction on a Bruker D8 Advance diffractometer (CuK_α radiation) in the angular range $2\theta = 10°–80°$.

Small-angle and ultrasmall-angle neutron scattering (SANS and USANS) measurements were performed at room temperature on the KWS-2 and KWS-3 diffractometers, respectively (FRM-II reactor, Garching, Germany) [31, 32]. The measurements on the KWS-2 instrument were made at a neutron wavelength $\lambda = 4.48$ Å ($\Delta\lambda/\lambda = 0.1$) in the momentum transfer range $5 \times 10^{-3} < q < 0.3$ Å^{-1}. The measurements on the KWS-3 were made at a neutron wavelength $\lambda = 12.8$ Å ($\Delta\lambda/\lambda = 0.2$) in the momentum transfer range $3 \times 10^{-4} < q < 3 \times 10^{-3}$ Å^{-1}. Before the measurements, thoroughly ground SiO_2 aerogel samples were placed between two quartz glass slides. The raw spectra in each q interval were corrected by a standard procedure [33] with allowance for the scattering by the accessories of the diffractometer and the cuvette and the room background. The two-dimensional isotropic spectra thus obtained were azimuthally averaged with allowance for the detector efficiency. In preliminary data processing, we used the QtiKWS program [34].

Table 1. Synthesis conditions and key properties of the SiO_2 aerogel samples

Solvent	t_c, °C	t_{drying}, °C	S, m^2/g	V_{pore}*, cm^3/g
Ethanol	243	210	580 ± 40	1.51 ± 0.05
		240	460 ± 30	0.85 ± 0.05
		260	470 ± 30	0.70 ± 0.04
HFIP	182	160	730 ± 50	1.67 ± 0.05
		190	690 ± 50	1.47 ± 0.05
		220	720 ± 50	1.31 ± 0.05

* The specific pore volume was evaluated from the limiting filling ($P/P_0 = 0.95$) [37].

RESULTS AND DISCUSSION

In all cases, by removing the solvents (ethanol and HFIP) we obtained monolithic aerogel samples which had a geometric density in the range ~0.2–0.3 g/cm^3. According to X-ray diffraction data, the samples were amorphous, which is typical of SiO_2 aerogels. ~~Note that t~~he ~~peak~~ position of the halo in the X-ray diffraction patterns of the samples prepared in HFIP was shifted to larger angles in comparison with that for the samples prepared in ethanol ($2\theta \sim 23°$ and 20°, respectively).

According to X-ray microanalysis data, all of the aerogel samples contained fluorine (the F : Si molar ratio was 0.12–0.17 and 0.5–0.7 in the aerogels prepared using ethanol and HFIP, respectively). The solvent removal temperature had essentially no effect on the fluorine content. The presence of fluorine was due to the use of hydrofluoric acid as a catalyst for TEOS hydrolysis. In the case of the aerogels prepared in the presence of HFIP, it was also due to the chemical modification of the silicon oxide matrix by fluorine-containing organic groups [35].

The thermal analysis data in Fig. 1 indicate that the thermolysis of the aerogels includes two main steps. One of them, taking place at temperatures below 150°C, is the removal of the physically bound water and organic solvents persisting in the aerogel matrix. The other thermal decomposition step, which begins at ~250°C and reaches completion at temperatures above 700°C, is the removal of the hydroxyl groups and organic compounds chemically bound to the SiO_2 matrix. The prominent exothermic peaks observed in the temperature range 250–400°C correspond to the oxidation of organic groups and confirm the chemical modification of the SiO_2 surface observed previously in analogous systems under high-temperature drying conditions [35, 36]. At the same time, on the whole the thermal behavior of the aerogels depends little on the solvent removal temperature.

Table 1 summarizes the microstructural characteristics (specific surface area and specific pore volume) of the samples, determined by low-temperature nitrogen adsorption measurements.

It can be seen from the data in Table 1 that, varying the solvent removal temperature in the specified range, one can obtain aerogels with a rather large specific surface area (500–700 m^2/g). Note that these data are consistent with previous results, which demonstrate that synthesis with HFIP as a solvent can yield aerogels with a larger specific surface area than in the case of lower aliphatic alcohols [38].

It also follows from the above data that removing the solvent below the critical temperature leads to the formation of materials that have an even larger specific surface area and higher porosity than in the case of drying under supercritical conditions. The effect is more pronounced if ethanol is used as a solvent. The likely reason for this phenomenon is that the silica solubility in alcohols decreases with decreasing temperature. At relatively low temperatures, the rate of ~~recondensation~~ processes that lead to the aggregation and growth of SiO_2 particles in the course of gel drying [39, 40] should be slower than that under supercritical conditions. Note that there is currently very little data on silica solubility in aliphatic alcohols. The silica solubility in ethanol is known to increase with increasing temperature, reaching 194 mg/L at 200°C and 274 mg/L at 225°C. Such data were also reported for methanol and isopropanol [41, 42], but there seem to be no such data for HFIP.

Figure 2 shows nitrogen adsorption/desorption isotherms for all of the aerogel samples and the corresponding pore size distributions. It can be seen that the aerogels prepared under supercritical and subcritical conditions have, respectively, the lowest and highest specific adsorption and pore volume values. Note that the solvent removal temperature has a negligible effect on the peak position in the pore size distributions, which is 4–5 nm for both ethanol and HFIP.

Scanning electron microscopy data (Fig. 3) are consistent with the adsorption measurement results: the samples prepared in different solvents and at different temperatures have essentially identical microstructures and contain pores less than 100 nm in size.

As pointed out above, the possibility of obtaining monolithic aerogels with a large specific surface area is due to the absence of considerable capillary stress in the course of solvent removal from the pores of the gel matrix [43]. The capillary pressure on the liquid–vapor interface ($p_c = (2\gamma\cos\theta)/r$, where γ is the surface tension coefficient, θ is the contact angle, and r is the pore radius) [44] can reach a considerable level, leading to disintegration of the gel structure. The surface tension of a liquid drops markedly near its critical temperature [45, 46]. For example, the surface tension of

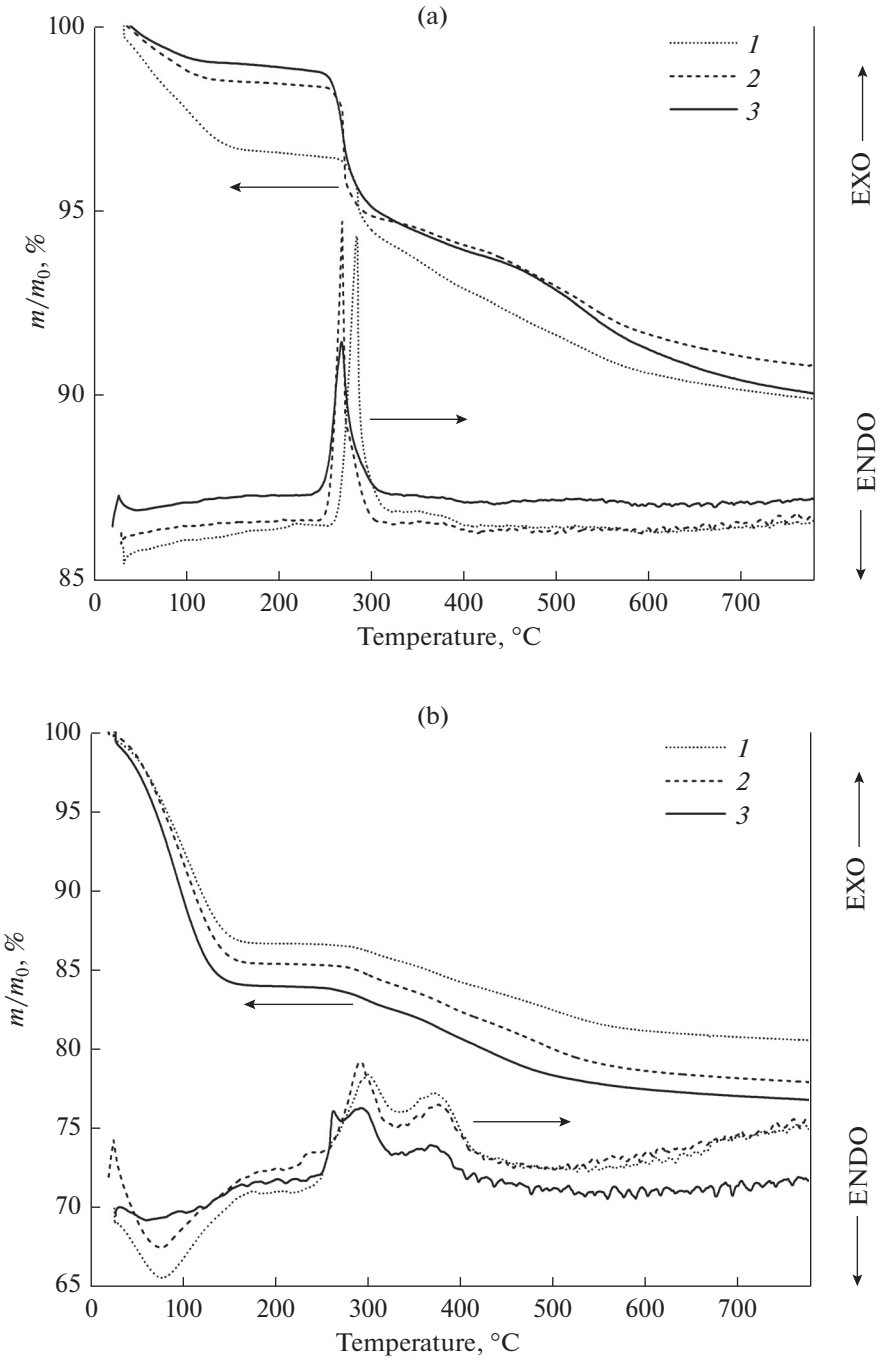

Fig. 1. Thermal analysis results for the SiO_2 aerogel samples prepared by removing (a) ethanol at temperatures of (*1*) 210, (*2*) 240, and (*3*) 260°C or (b) HFIP at temperatures of (*1*) 160, (*2*) 190, and (*3*) 220°C.

ethanol is about 2.3×10^{-2} N/m at 20°C, 3.3×10^{-3} N/m at 210°C, and 10^{-4} N/m at 240°C. It seems likely that the low surface tension of the solvents at temperatures 20–30°C below their critical temperature is responsible for the large specific surface area and monolithic state of the aerogels obtained in this study.

Figure 4 shows the experimentally determined differential macroscopic neutron scattering cross sections, $d\Sigma(q)/d\Omega$, for our SiO_2 aerogel samples. On the whole, all of the scattering curves are qualitatively similar, independent of the synthesis conditions.

The observed scattering pattern is typical of hierarchical structures [47] with different characteristic length scales and different types of aggregation at each structural level. To analyze the SANS and USANS data in detail, we used the unified exponential power-law equation [48]

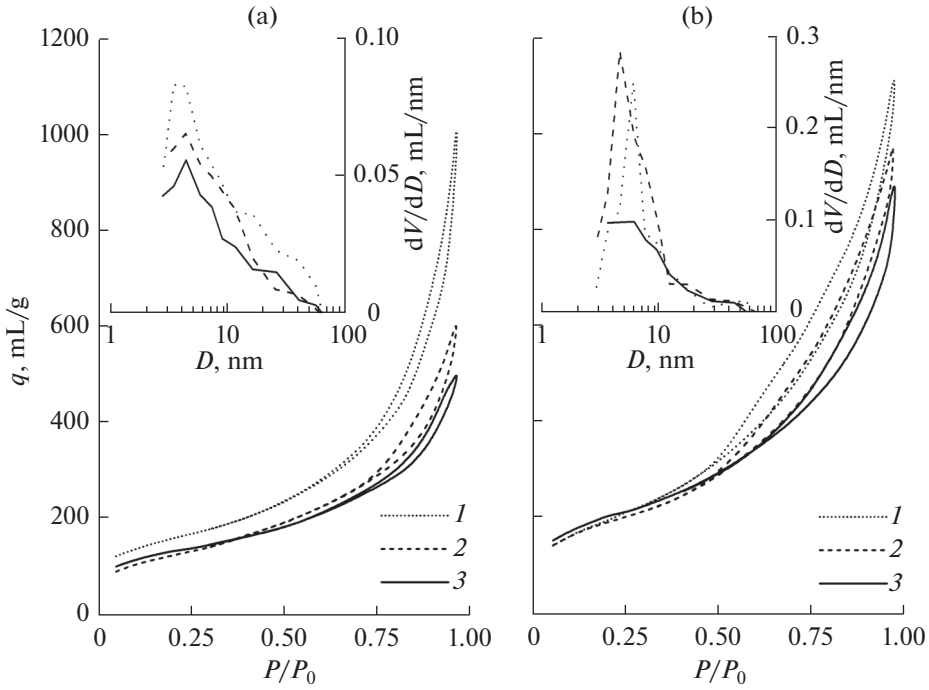

Fig. 2. Full nitrogen sorption/desorption isotherms and pore size distributions (insets) for the SiO_2 aerogel samples prepared by removing (a) ethanol at temperatures of (*1*) 210, (*2*) 240, and (*3*) 260°C or (b) HFIP at temperatures of (*1*) 160, (*2*) 190, and (*3*) 220°C.

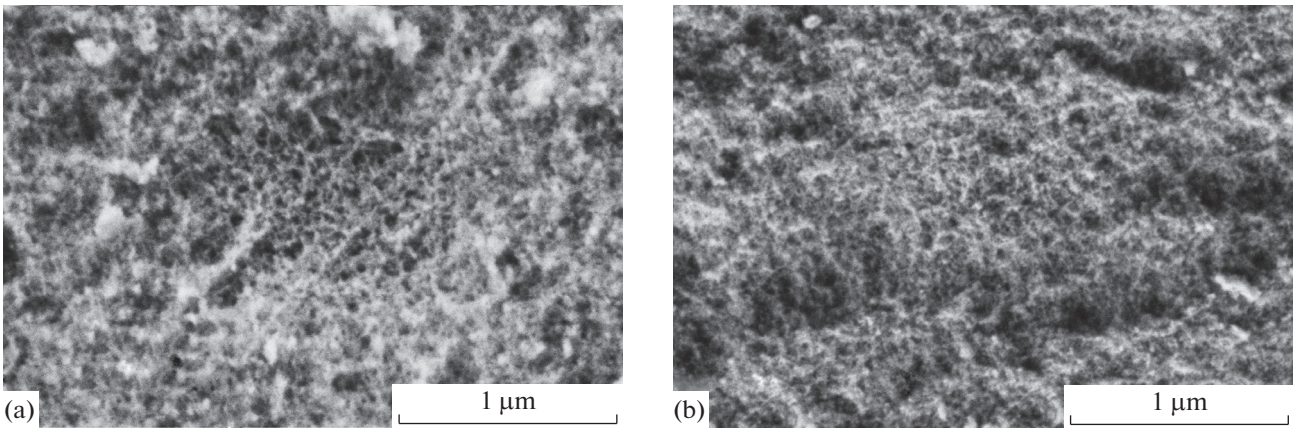

Fig. 3. Micrographs of the SiO_2 aerogels prepared by removing (a) ethanol at 240°C and (b) HFIP at 190°C.

$$\frac{d\Sigma(q)}{d\Omega} = \sum_{i=1}^{3}\left(G_i \exp\left(-\frac{q^2R_{gi}^2}{3}\right) + B_i \exp\left(-\frac{q^2R_{g(i-1)}^2}{3}\right)\left[\frac{(\mathrm{erf}(q\,R_{gi}/\sqrt{6}))}{q}\right]^{n_i}\right) + I_{inc}, \quad (1)$$

where G_i is the Guinier prefactor, R_{gi} is the radius of gyration of inhomogeneities, B_i is the power-law prefactor, the exponent n_i depends on the nature of particle aggregation, and the constant I_{inc} is associated with incoherent scattering by hydrogen atoms. The summation in relation (1) is carried out over three structural levels (i). To obtain final results, relation (1) was convoluted with the instrument resolution function. The experimental $d\Sigma(q)/d\Omega$ differential scattering cross section data were analyzed using least squares fitting. The data processing results are presented in Fig. 4 (continuous lines) and Table 2.

The data presented in Table 2 demonstrate that all of the aerogels are fractal systems with a three-level hierarchical structure and that the synthesis conditions (the nature of the solvent and the drying temperature) influence its parameters.

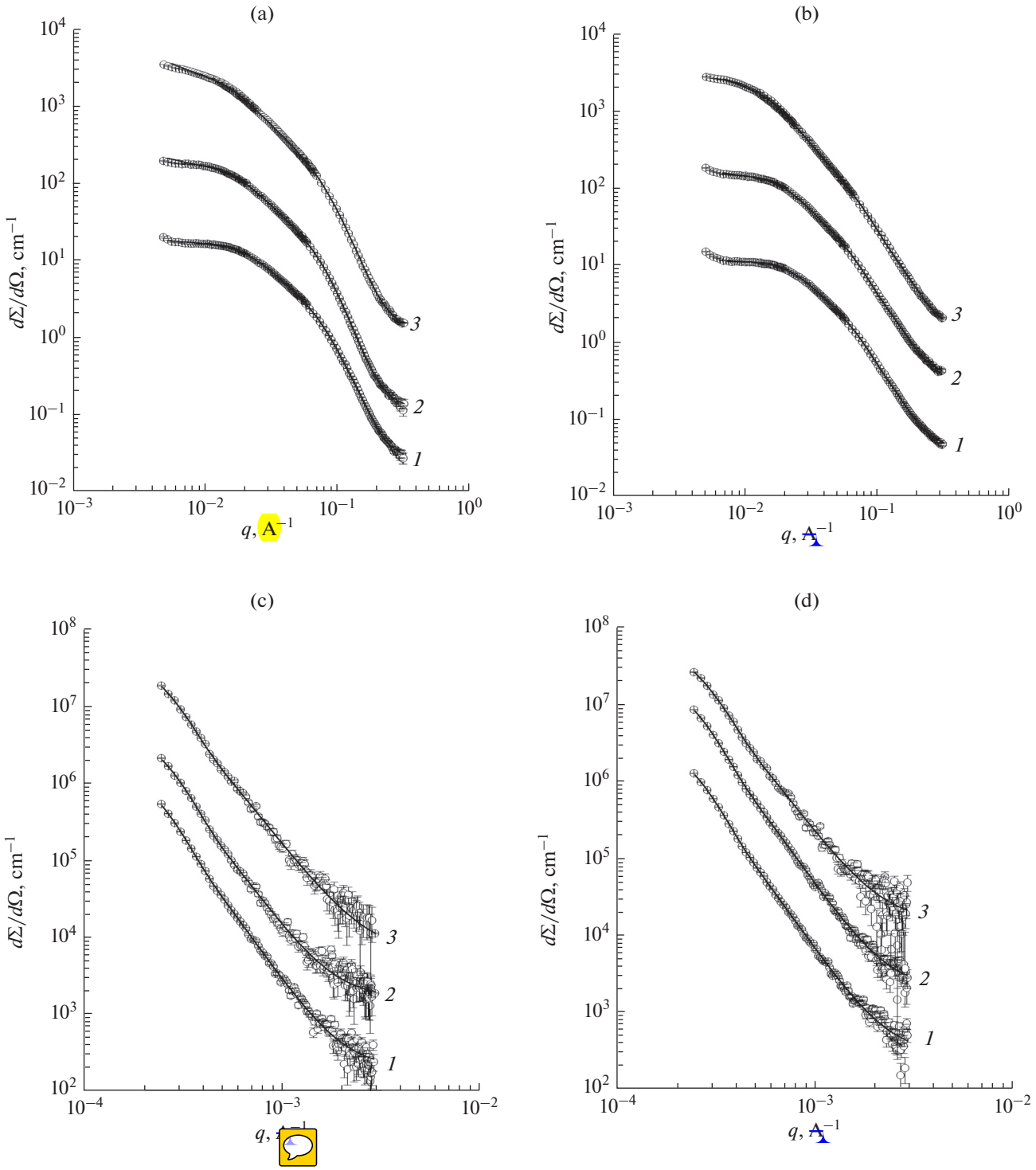

Fig. 4. Differential neutron scattering cross section dΣ(*q*)/dΩ as a function of momentum transfer *q* for the aerogel samples prepared using (a, c) ethanol at temperatures of (*1*) 210, (*2*) 240, and (*3*) 260°C or (b) HFIP at temperatures of (*1*) 160, (*2*) 190, and (*3*) 220°C: (a, b) SANS and (c, d) USANS data. For clarity, the dΣ(*q*)/dΩ values in curves *2* and *3* are multiplied by 10 and 100, respectively.

The structure of the aerogels prepared using ethanol is characterized by the presence of clusters (the first structural level) with a characteristic size R_{g1} (the upper self-similarity limit) in the range 2.3–2.6 nm and a relatively small surface area, characterized by a fractal dimension (D_{s1}) not exceeding 2.5. The clusters form mass fractal aggregates (second structural level) with a fractal dimension from 1.5 to 1.8 and a charac-

Table 2. Mesostructure parameters of the SiO_2 aerogels as evaluated from analysis of USANS and SANS data (the parameters G_i, B_i, and I_{inc} are omitted).

Solvent	Ethanol			HFIP		
T_{drying}, °C	210	240	260	160	190	220
1st structural level (SANS data)						
R_{g1}, Å	23.1 ± 0.7	25.5 ± 0.5	23.7 ± 0.7	20.5 ± 0.7	20.5 ± 1.5	17.9 ± 0.5
$D_{s1} = 6 - n_1$	2.3 ± 0.2	2.1 ± 0.1	2.14 ± 0.09	–		
$D_{m1} = n_1$	–			2.65 ± 0.07	2.66 ± 0.08	2.7 ± 0.07
2nd structural level (SANS data)						
R_{g2}, Å	175 ± 7	220 ± 4	233 ± 6	149 ± 2	176 ± 6	231 ± 3
$D_{m2} = n_2$	1.55 ± 0.06	1.68 ± 0.06	1.83 ± 0.03	1.69 ± 0.05	1.81 ± 0.06	2.05 ± 0.03
3rd structural level (USANS data)						
R_{g3}, μm	0.96 ± 0.05	0.88 ± 0.04	0.89 ± 0.04	0.91 ± 0.04	0.90 ± 0.04	0.83 ± 0.04
$D_{s3} = 6 - n_3$	2.38 ± 0.02	2.44 ± 0.05	2.62 ± 0.04	2.37 ± 0.06	2.47 ± 0.03	2.65 ± 0.03

teristic size R_{g2} = 17–23 nm. Raising the gel drying temperature leads to a systematic increase in the size of the aggregates of the second structural level, which seems to account for the observed reduction in the specific surface area of the aerogels (Table 1).

The first structural level of the aerogels prepared using HFIP is characterized by the presence of rather dense mass fractal clusters (fractal dimension, 2.6–2.7) with a characteristic size in the range 1.8–2 nm. Cluster aggregates also have a mass fractal structure ($1.69 \le D_{m2} \le 2.05$) and possess a somewhat smaller characteristic size (15–23 nm) in comparison with the aerogels prepared using ethanol (17–23 nm).

The third structural level of all the aerogel obtained in this study corresponds to large agglomerates with a characteristic size $R_{g3} \approx 1$ μm, possessing a large fractal surface area with a dimension in the range 2.37–2.65, which increases systematically with increasing gel drying temperature.

CONCLUSIONS

Using low-temperature nitrogen adsorption measurements, X-ray diffraction, thermal analysis, scanning electron microscopy, X-ray microanalysis, and small-angle and ultrasmall-angle neutron scattering, we have carried out the first comparative analysis of the physicochemical characteristics of SiO_2 aerogels prepared by drying under subcritical and supercritical conditions. The results demonstrate that aerogel synthesis at temperatures 20–30°C below the critical temperature of the solvent (ethanol or hexafluoroisopropanol) yields materials that are characterized by higher specific porosity in comparison with the aerogels obtained under supercritical conditions and have the same or a larger specific surface area. The nature of the solvent used and the solvent removal temperature have a significant effect on the size and aggregation behavior of primary SiO_2 clusters and the cluster aggregate size. The structural parameters of the SiO_2 aerogels seem to be determined by the temperature dependence of the silica solubility in the alcohols and the temperature dependence of the surface tension of the alcohols in the near-critical region.

The present results pave the way to energy-efficient processes for the preparation of functional and structural oxide aerogel-based materials.

ACKNOWLEDGMENTS

This work was supported by the Russian Science Foundation (grant no. 14-13-01150) and was carried out using equipment ~~at the Shared Physical Characterization Facilities Center~~, Kurnakov Institute of General and Inorganic Chemistry, Russian Academy of Sciences.

REFERENCES

1. Kim, J., Nakanishi, H., Pollanen, J., Smoukov, S., Halperin, W.P., and Grzybowski, B.A., Nanoparticle-loaded aerogels and layered aerogels cast from sol–gel mixtures, *Small,* 2011, vol. 7, no. 18, pp. 2568–2572.
2. *Nanomaterialy: Svoistva i perspektivnye primeneniya (Properties and Potential Applications of Nanomaterials)*, Yaroslavtsev, A.B., Ed., Moscow: Nauchnyi Mir, 2014.
3. Schmidt, M. and Schwertfeger, F., Applications for silica aerogel products, *J. Non-Cryst. Solids,* 1998, vol. 225, pp. 364–368.
4. Anderson, M.L., Stroud, R.M., Morris, C.A., Merzbacher, C.I., and Rolison, D.R., Tailoring advanced nanoscale materials through synthesis of composite

aerogel architectures, *Adv. Eng. Mater.,* 2000, vol. 2, no. 8, pp. 481–488.

5. Pajonk, G.M., Catalytic aerogels, *Catal. Today,* 1997, vol. 35, no. 3, pp. 319–337.
6. Melde, B.J., Johnson, B.J., and Charles, P.T., Mesoporous silicate materials in sensing, *Sensors,* 2008, vol. 8, no. 8, pp. 5202–5228.
7. He, Y.L. and Xie, T., Advances of thermal conductivity models of nanoscale silica aerogel insulation material, *Appl. Thermal Eng.,* 2015, vol. 81, pp. 28–50.
8. Pierre, A.C. and Pajonk, G.M., Chemistry of aerogels and their applications, *Chem. Rev.,* 2002, vol. 102, no. 11, pp. 4243–4266.
9. Gurav, J.L., Jung, I.K., Park, H.H., Kang, E.S., and Nadargi, D.Y., Silica aerogel: synthesis and applications, *J. Nanomater.,* 2010, vol. 2010, paper 409 310.
10. Moretti, A., Maroni, F., Osada, I., Nobili, F., and Passerini, S., V_2O_5 aerogel as a versatile cathode material for lithium and sodium batteries, *ChemElectroChem,* 2015, vol. 2, no. 4, pp. 529–537.
11. Balakhonov, S.V., Vatsadze, S.Z., and Churagulov, B.R., Effect of supercritical drying parameters on the electrochemical properties of vanadium oxide-based aerogels, *Inorg. Mater.,* 2017, vol. 53, no. 2, pp. 181–184.
12. Campbell, L.K., Na, B.K., and Ko, E.I., Synthesis and characterization of titania aerogels, *Chem. Mater.,* 1992, vol. 4, no. 6, pp. 1329–1333.
13. Yao, N., Cao, S., and Yeung, K.L., Mesoporous TiO_2–SiO_2 aerogels with hierarchal pore structures, *Microporous Mesoporous Mater.,* 2009, vol. 117, no. 3, pp. 570–579.
14. Luo, L., Cooper, A.T., and Fan, M., Preparation and application of nanoglued binary titania–silica aerogel, *J. Hazard. Mater.,* 2009, vol. 161, no. 1, pp. 175–182.
15. Yorov, Kh.E., Sipyagina, N.A., Malkova, A.N., Baranchikov, A.E., Lermontov, S.A., Borilo, L.P., and Ivanov, V.K., Methyl *tert*-butyl ether as a new solvent for the preparation of SiO_2–TiO_2 binary aerogels, *Inorg. Mater.,* 2016, vol. 52, no. 2, pp. 163–169.
16. Gavrilov, A.I., Balakhonov, S.V., and Churagulov, B.R., Synthesis and photocatalytic activity of anatase-based aerogels, *Inorg. Mater.*, 2016, vol. 52, no. 12, pp. 1240–1243.
17. Miller, J.B., Rankin, S.E., and Ko, E.I., Strategies in controlling the homogeneity of zirconia–silica aerogels: effect of preparation on textural and catalytic properties, *J. Catal.,* 1994, vol. 148, no. 2, pp. 673–682.
18. Pekala, R.W., Alviso, C.T., Kong, F.M., and Hulsey, S.S., Aerogels derived from multifunctional organic monomers, *J. Non-Cryst. Solids,* 1992, vol. 145, pp. 90–98.
19. Shea, K.J. and Loy, D.A., Bridged polysilsesquioxanes. Molecular-engineered hybrid organic–inorganic materials, *Chem. Mater.,* 2001, vol. 13, no. 10, pp. 3306–3319.
20. Gui, X., Wei, J., Wang, K., Cao, A., Zhu, H., Jia, Y., and Wu, D., Carbon nanotube sponges, *Adv. Mater.,* 2010, vol. 22, no. 5, pp. 617–621.
21. Worsley, M.A., Pauzauskie, P.J., Olson, T.Y., Biener, J., Satcher, J.H., Jr., and Baumann, T.F., Synthesis of graphene aerogel with high electrical conductivity, *J. Am. Chem. Soc.,* 2010, vol. 132, no. 40, pp. 14067–14069.
22. Mazraeh-shahi, Z.T., Shoushtari, A.M., Abdouss, M., and Bahramian, A.R., Relationship analysis of processing parameters with micro and macro structure of silica aerogel dried at ambient pressure, *J. Non-Cryst. Solids,* 2013, vol. 376, pp. 30–37.
23. Omranpour, H. and Motahari, S., Effects of processing conditions on silica aerogel during aging: role of solvent, time and temperature, *J. Non-Cryst. Solids,* 2013, vol. 379, pp. 7–11.
24. Rao, A.V., Bhagat, S.D., Hirashima, H., and Pajonk, G.M., Synthesis of flexible silica aerogels using methyltrimethoxysilane (MTMS) precursor, *J. Colloid Interface Sci.,* 2006, vol. 300, no. 1, pp. 279–285.
25. Zhou, X., Zhong, L., and Xu, Y., Surface modification of silica aerogels with trimethylchlorosilane in the ambient pressure drying, *Inorg. Mater.,* 2008, vol. 44, no. 9, pp. 976–979.
26. Kirkbir, F., Murata, H., Meyers, D., and Chaudhuri, S.R., Drying of aerogels in different solvents between atmospheric and supercritical pressures, *J. Non-Cryst. Solids,* 1998, vol. 225, pp. 14–18.
27. Yoda, S. and Ohshima, S., Supercritical drying media modification for silica aerogel preparation, *J. Non-Cryst. Solids,* 1999, vol. 248, no. 2, pp. 224–234.
28. Tajiri, K., Igarashi, K., and Nishio, T., Effects of supercritical drying media on structure and properties of silica aerogel, *J. Non-Cryst. Solids,* 1995, vol. 186, pp. 83–87.
29. Lermontov, S.A., Straumal, E.A., Mazilkin, A.A., Zverkova, I.I., Baranchikov, A.E., Straumal, B.B., and Ivanov, V.K., How to tune the alumina aerogels structure by the variation of a supercritical solvent. Evolution of the structure during heat treatment, *J. Phys. Chem. C,* 2016, vol. 120, no. 6, pp. 3319–3325.
30. Wang, S., Raychaudhuri, S., and Sarkar, A., US Patent 5 264 197, 1993.
31. Radulescu, A., Kentzinger, E., Stellbrink, J., Dohmen, L., Alefeld, B., Rücker, U., and Richter, D., KWS-3: the new (very) small-angle neutron scattering instrument based on focusing-mirror optics, *Neutron News,* 2005, vol. 16, no. 2, pp. 18–21.
32. Goerigk, G. and Varga, Z., Comprehensive upgrade of the high-resolution small-angle neutron scattering instrument KWS-3 at FRM II, *J. Appl. Crystallogr.,* 2011, vol. 44, no. 2, pp. 337–342.
33. Wignall, G.D.T. and Bates, F.S., Absolute calibration of small-angle neutron scattering data, *J. Appl. Crystallogr.,* 1987, vol. 20, no. 1, pp. 28–40.
34. www.iff.kfa-juelich.de/~pipich/doku-wiki/doku.php/qtikws.
35. Lermontov, S., Malkova, A., Yurkova, L., Straumal, E., Gubanova, N., Baranchikov, A., Smirnov, M., Tarasov, V., Buznik, V., and Ivanov, V., Hexafluoroisopropyl alcohol as a new solvent for aerogels preparation, *J. Supercrit. Fluids,* 2014, vol. 89, pp. 28–32.
36. Lermontov, S.A., Malkova, A.N., Sipyagina, N.A., Baranchikov, A.E., Petukhov, D.I., and Ivanov, V.K., Hydrophobicity/hydrophilicity control for SiO_2-based aerogels: the role of a supercritical solvent, *Russ. J. Inorg. Chem.,* 2015, vol. 60, no. 10, pp. 1169–1172.

37. Lowell, S., Shields, J.E., Thomas, M.A., and Thommes, M., *Characterization of Porous Solids and Powders: Surface Area, Pore Size and Density,* Dordrecht: Kluwer Academic, 2012.

38. Lermontov, S.A., Malkova, A.N., Sipyagina, N.A., Baranchikov, A.E., Petukhov, D.I., and Ivanov, V.K., Hexafluoroacetone: a new solvent for manufacturing SiO_2-based aerogels, *Russ. J. Inorg. Chem.,* 2015, vol. 60, no. 5, pp. 541–545.

39. *Nanoscale Materials in Chemistry,* Klabunde, K.J. and Richards, R.M., Eds., New York: Wiley, 2009, p. 213.

40. Hüsing, N. and Schubert, U., Aerogels—airy materials: chemistry, structure, and properties, *Angew. Chem., Int. Ed.,* 1998, vol. 37, pp. 22–45.

41. Kitahara, S., Dissolution of heat-treated silica gel powders in alcohols at 100° to 250°C, *Nippon Kagaku Zasshi,* 1969, vol. 90, no. 3, pp. 237–241.

42. Asano, T. and Kitahara, S., The dissolution of heat-treated silica gel powders and change of their surface induced by treatment with methanol at 150–250°C, *Nippon Kagaku Zasshi,* 1970, vol. 91, no. 2, pp. 109–117.

43. Deshpande, R., Hua, D.-W., Smith, D.M., and Brinker, C.J., Pore structure evolution in silica gel during aging/drying. III. Effects of surface tension, *J. Non-Cryst. Solids,* 1992, vol. 144, pp. 32–44.

44. Bear, J., *Dynamics of Fluids in Porous Media,* New York: American Elsevier, 1972.

45. Vargaftik, N.B., *Spravochnik po teplofizicheskim svoistvam gazov i zhidkostei (Thermophysical Properties of Gases and Liquids: A Handbook)*, Moscow: Nauka, 1972.

46. Volyak, L.D., Equations for evaluating the surface tension of liquids, *Teploenergetika,* 1958, no. 7, pp. 33–37.

47. *Hybrid organic–inorganic composites,* Mark, J.E., Lee, C.Y.-C., and Bianconi, P.A., Eds., Washington DC: American Chemical Society, 1995, pp. 97–111.

48. Beaucage, G., Approximations leading to a unified exponential power-law approach to small-angle scattering, *J. Appl. Crystallogr.,* 1995, vol. 28, pp. 717–728.

Translated by O. Tsarev

SPELL: 1. OK